PLOS ONE

RESEARCH ARTICLE

TRPM8 modulates temperature regulation in a sex-dependent manner without affecting cold-induced bone loss

Adriana Lelis Carvalho[1], Annika Treyball[1], Daniel J. Brooks[2], Samantha Costa[1], Ryan J. Neilson[1], Michaela R. Reagan[1,3,4], Mary L. Bouxsein[2,5], Katherine J. Motyl[1,3,4]*

1 Center for Molecular Medicine, Maine Medical Center Research Institute, Scarborough, ME, United States of America, **2** Center for Advanced Orthopaedic Studies, Beth Israel Deaconess Medical Center, Boston, MA, United States of America, **3** Tufts University School of Medicine, Tufts University, Boston, MA, United States of America, **4** Graduate School of Biomedical Sciences and Engineering, The University of Maine, Orono, ME, United States of America, **5** Department of Orthopedic Surgery, Harvard Medical School, Boston, MA, United States of America

* motylk@mmc.org

Citation: Lelis Carvalho A, Treyball A, Brooks DJ, Costa S, Neilson RJ, Reagan MR, et al. (2021) TRPM8 modulates temperature regulation in a sex-dependent manner without affecting cold-induced bone loss. PLoS ONE 16(6): e0231060. https://doi.org/10.1371/journal.pone.0231060

Editor: Josep A. Villena, Vall d'Hebron Institut de Recerca, SPAIN

Received: March 6, 2020

Accepted: May 6, 2021

Published: June 4, 2021

Data Availability Statement: All relevant data are within the paper and its Supporting Information files.

Funding: NIH/NIAMS K01AR067858 to Katherine Motyl, PhD, Principal Investigator. NIH/NIGMS P20GM121301 to Katherine Motyl, PhD, Project Leader, and Michaela Reagan, PhD, Project Leader. NIH/NCI R37CA245330 to Michaela Reagan, PhD, Principal Investigator. The funders had no role in study design, data collection and analysis, decision to publish, or preparation of the manuscript.

Abstract

Trpm8 (transient receptor potential cation channel, subfamily M, member 8) is expressed by sensory neurons and is involved in the detection of environmental cold temperatures. TRPM8 activity triggers an increase in uncoupling protein 1 (*Ucp1*)-dependent brown adipose tissue (BAT) thermogenesis. Bone density and marrow adipose tissue are both influenced by rodent housing temperature and brown adipose tissue, but it is unknown if TRPM8 is involved in the co-regulation of thermogenesis and bone homeostasis. To address this, we examined the bone phenotypes of one-year-old *Trpm8* knockout mice (*Trpm8-KO*) after a 4-week cold temperature challenge. Male *Trpm8-KO* mice had lower bone mineral density than WT, with smaller bone size (femur length and cross-sectional area) being the most striking finding, and exhibited a delayed cold acclimation with increased BAT expression of *Dio2* and *Cidea* compared to WT. In contrast to males, female *Trpm8-KO* mice had low vertebral bone microarchitectural parameters, but no genotype-specific alterations in body temperature. Interestingly, *Trpm8* was not required for cold-induced trabecular bone loss in either sex, but bone marrow adipose tissue in females was significantly suppressed by *Trpm8* deletion. In summary, we identified sex differences in the role of TRPM8 in maintaining body temperature, bone microarchitecture and marrow adipose tissue. Identifying mechanisms through which cold temperature and BAT influence bone could help to ameliorate potential bone side effects of obesity treatments designed to stimulate thermogenesis.

Introduction

Maintaining body temperature homeostasis involves both the regulation of heat loss and generation of heat (i.e. thermogenesis). Mammals require energy to generate and conserve heat when in temperatures below their thermoneutral zone, which is room temperature in humans,

Competing interests: The authors have declared that no competing interests exist.

and warmer (28–32˚C) in mice [1]. During adaptation to cooler temperatures, sympathetic nervous system (SNS) output increases, elevating energy expenditure, fat oxidation, and heat production by brown adipose tissue (BAT). Uncoupling protein 1 (*Ucp1*) in the inner mitochondrial membrane of BAT generates heat by uncoupling oxidative phosphorylation from ATP production [2, 3]. In addition, cold exposure can also trigger white adipose tissue (WAT) beiging to enhance heat production [4]. Previous studies have demonstrated a relationship between SNS activity and the skeleton, revealing that sympathetic outflow is not only involved in the activation of BAT thermogenesis for thermoregulation purposes, but that sympathetic tone can also suppress bone formation by signaling through the β2-adrenergic receptor (β2AR) expressed by osteoblasts [5, 6]. Marrow adipocytes share a common mesenchymal precursor with osteoblasts and are known to be elevated in many conditions of low bone density. The SNS suppresses both bone formation and bone marrow adipose tissue (BMAT), and a four-week cold exposure in one-year-old C3H/HeJ mice reduced BMAT at the most active sites of bone remodeling [7]. In that study, however, bone parameters were largely unchanged, and there was no indication of whether C57BL/6J mice (a commonly used model for skeletal research) would have bone loss from cold challenge. More recent studies, however, showed that thermoneutral (32˚C) housing in C57BL/6J mice exerted a protective effect on the skeleton, which was associated with reduced expression of *Ucp1* in BAT [1, 8]. Interestingly, the non-selective β-blocker propranolol was recently shown to be protective against adipose tissue loss, but only partly protective against bone loss, in mice housed at room temperature compared to thermoneutrality [9]. It is clear that cold temperature influences bone and marrow adipose tissue, but what particular afferent thermoregulatory pathways may be involved in these processes is unknown.

Transient receptor potential melastatin 8 (TRPM8) is a Ca^{2+} permeable, non-selective cation channel expressed by temperature-sensing sensory neurons and is known to be the principal detector of innocuous cold [10]. In mice, TRPM8 is activated by a wide temperature range, approximately between 28˚C to 8˚C, and also by cooling agents (e.g. menthol and icilin) [11]. Previously, TRPM8 was primarily described to work as a peripheral thermal sensor; however, there is evidence that this cold-sensing channel is also involved in thermoregulation by promoting heat conservation and energy homeostasis [12]. Furthermore, TRPM8 is a potential target for obesity treatment due to its function in regulating energy metabolism [12–17]. TRPM8 can trigger non-shivering thermogenesis in BAT and the beiging of WAT in mice [17, 18] and humans [15]. Moreover, *Trpm8* knockout (*Trpm8*-KO) mice are hyperphagic and have reduced fat oxidation when housed at 21˚C, promoting the development of obesity [12]. However, it is unknown whether TRPM8 has a role in regulating bone density *in vivo* and by inference, whether modulation of TRPM8 by obesity therapeutics might influence bone.

Thus, we conducted this study to determine whether the cold-sensing TRPM8 channel would be required for any cold-induced changes in the skeleton and bone marrow adipose tissue. We hypothesized that *Trpm8* deletion would impair body temperature regulation but may protect mice from cold-induced bone loss and marrow adipose tissue changes. We challenged one-year-old male and female WT and *Trpm8* knockout (KO) mice to cold temperature housing (4˚C) and examined body temperature, peripheral and marrow adipose tissue, and bone microarchitecture and turnover. We found that male *Tprm8-KO* mice had impaired temperature regulation while females did not. Male *Trpm8-KO* mice had a more overt low bone density phenotype, but females also had reduced microarchitectural parameters in femoral cortical bone and vertebral trabecular bone. Overall, cold temperature reduced trabecular bone volume fraction in males, while reducing cortical area fraction in females, but these effects were not dependent upon genotype. Surprisingly, bone marrow adiposity was lower in *Trpm8-KO* females compared to WT, but there was no significant effect of cold on BMATin

either genotype or sex of mice. There were, however, sex and genotype specific effects on the utilization of peripheral adipose tissue stores, suggesting TRPM8 regulates thermogenic tissues in a sex-dependent manner.

Materials and methods

Mice

B6.129P2-*Trpm8*^{tm1Jul}/J mice (*Trpm8-knockout (Trpm8-KO*) were purchased from The Jackson Laboratory (stock #008198) and bred to C57BL/6J mice to generate heterozygous mice. *Trpm8-KO* and *Wild-type* (WT) littermate control mice were generated from heterozygous matings. Mice were bred and housed in a barrier animal facility at Maine Medical Center Research Institute (MMCRI) on a 14-hr light and 10-hr dark cycle. Male and female, WT and *Trpm8-KO* (N = 14-19/group) mice were aged to 52 weeks while being housed up to four animals per cage at 22˚C before initiating the cold challenge (below). Mice were given water and chow (Teklad global 18% protein diet, #2918, Envigo) *ad libitum*. Mice were housed with Alphi Dri Plus bedding (Shepherd Specialty Papers), which allowed the mice to build small nests. All animal protocols in this study were approved by the Institutional Animal Care and Use Committee (IACUC) of MMCRI, an Association for Assessment and Accreditation of Laboratory Animal Care (AAALAC)-accredited facility. Mice were monitored daily for any signs of pain and distress. Except as detailed below in the "Cold housing study" section, anesthesia and other steps to minimize pain and distress were not needed because mice did not exhibit any signs. Euthanasia was performed using isoflurane anesthesia followed by cervical dislocation or decapitation. Experiments were performed in four independent cohorts of mice.

Dual-energy X-ray absorptiometry (DXA)

All mice had body weight measured prior to DXA. Mice underwent isoflurane anesthesia for DXA scanning, and were monitored following removal of anesthesia until they were awake and fully ambulatory in cages. Areal bone mineral content (aBMC), bone mineral density (aBMD), lean mass and fat mass measurements were performed on each mouse by a PIXImus dual energy X-ray densitometer (GE Lunar, GE Healthcare). The PIXImus was calibrated daily with a mouse phantom provided by the manufacturer. Mice were ventral side down with each limb and tail positioned away from the body. Full-body scans were obtained, and the head was excluded from analyses because of concentrated mineral content in skull and teeth. DXA data were processed and analyzed with Lunar PIXImus 2 (version 2.1) software [19]. Adiposity index was defined as fat mass divided by fat-free mass. DXA measurements were only performed before cold housing because we could not bring mice back into our barrier animal facility after cold housing outside of the barrier.

Cold housing study

Fifty-two week-old, male and female, WT and *Trpm8-KO* mice were separated into individual cages. Half of the mice were maintained at room temperature (N = 7-8/group), while the other half were moved to a cold room (N = 6-11/group) with automatic lights set to a 14 hr light, 10 hr dark cycle, equivalent to the light schedule of room temperature mice. We used a Thorlabs, Inc. (Newton, NJ) PM100USB Power and Energy Meter to detect the intensity of the visible light in each room. The range of light intensity was comparable between rooms, with a range of 80–160 μW in the room temperature room and a range of 80–200 μW in the cold room, depending upon location of the mouse cage. Mice were randomly placed on shelves, such that no specific genotype or sex was always in the same place. Cold-treated mice were acclimatized

to 18˚C for 1 week, then 4˚C for 3 weeks. This method of cold-temperature exposure has been previously published to produce changes in marrow adipose tissue C3H/HeJ mice and in C57BL/6J mice as well as used to determine dependence of cold-acclimation on energy expenditure in mice [7, 20]. Rectal temperature was measured daily in cold room mice and every 2 hours on the day of change to 4˚C with a Type T thermocouple rectal probe (RET-3, Physitemp Instruments, Inc., Clifton, NJ, USA) with a MicroTherma 2T hand-held thermometer (ThermoWorks, Inc., Lindon, UT; cat. no. THS-227-193). Cages contained standard bedding. Mice were fed regular chow and water *ad libitum*. Environmental temperature and humidity was measured and recorded daily. Mice were monitored for signs of pain and distress twice per day and every 2 hours on the day of change to 4˚C. We monitored and recorded any of the following signs: shivering, hunched posture, reduced mobility, ruffled fur and vocalization. Signs that were found included occasional shivering and ruffled fur, and these generally resolved immediately if not associated with low core temperature. If core temperature fell below 30˚C, mice were immediately removed to room temperature and euthanized. No mice exhibited temperatures below this threshold or exhibited signs of distress during the transition from 18˚C to 4˚C. During the 4˚C period, two mice (one male +/+ and one male -/-) exhibited a low body temperature and were immediately euthanized following isoflurane anesthesia. No mice died spontaneously.

Histology

Femur and all adipose tissue samples were placed in 10% neutral buffered formalin (Sigma-Aldrich) for 48 hr and then stored in 70% ethanol. Bones were decalcified with EDTA and bone and adipose tissue samples were paraffin embedded and tissues sections of 5 μm were deparaffinized and rehydrated in a graded series (100–70%) of ethanol washes and stained with hematoxylin and eosin (H&E). Photomicrographs of H&E stained tissues were taken at 4x magnification.

Bone marrow adipocyte quantification

A blinded analysis of bone marrow (BM) adipocytes was performed on each histology slide using ImageJ software (https://imagej.nih.gov/ij/). A global scale was set at 1000 pixels/mm based on the microscope imaging objective and settings. The tissue area (T.Ar) was selected in the distal femoral metaphysis (0.1 mm proximal to the epiphyseal growth plate) using the polygon tool to contain the BM, excluding cortical bone. One histological slide per distal femur was measured. The T.Ar was measured using ImageJ to find the total tissue area, which was used to normalize adipocyte numbers (Ad.N) per T.Ar for each image. Ad.N was measured manually.

Micro-computed tomography (μCT)

A high-resolution desktop micro-tomographic imaging system (μCT40, Scanco Medical AG, Brüttisellen, Switzerland) was used to assess trabecular bone architecture in the distal femoral metaphysis and L5 vertebral body and cortical bone morphology of the femoral mid-diaphysis. Scans were acquired using a 10 μm^3 isotropic voxel size, 70 kVP, 114 μA, 200 ms integration time, and were subjected to Gaussian filtration and segmentation. Image acquisition and analysis protocols adhered to guidelines for the assessment of rodent bones by μCT [21]. In the femur, trabecular bone microarchitecture was evaluated in a 1500 μm (150 transverse slices) region beginning 200 μm superior to the peak of the growth plate and extending proximally. In the L5 vertebral body, trabecular bone was evaluated in a region beginning 100 μm inferior to the cranial end-plate and extending to 100 μm superior to the caudal end-plate. The

trabecular bone regions were identified by manually contouring the endocortical region of the bone. Thresholds of 335 mgHA/cm^3 and 385 mgHA/cm^3 were used to segment bone from soft tissue in the femur and L5 vertebrae, respectively. The following architectural parameters were measured using the Scanco Trabecular Bone Morphometry evaluation script: trabecular bone volume fraction (Tb.BV/TV, %), trabecular bone mineral density (Tb. BMD, mgHA/cm^3), specific bone surface (BS/BV, mm^2/mm^3), trabecular thickness (Tb.Th, mm), trabecular number (Tb.N, mm^{-1}), and trabecular separation (Tb.Sp, mm), connectivity density (Conn.D, 1/mm^3). Cortical bone was assessed in 50 transverse μCT slices (500 μm long region) at the femoral mid-diaphysis and the region included the entire outer most edge of the cortex. Cortical bone was segmented using a fixed threshold of 708 mgHA/cm^3. The following variables were computed: total cross-sectional area (bone + medullary area) (Tt.Ar, mm^2), cortical bone area (Ct. Ar, mm^2), medullary area (Ma.Ar, mm^2), bone area fraction (Ct.Ar/Tt.Ar, %), cortical tissue mineral density (Ct.TMD, mgHA/cm^3), cortical thickness (Ct.Th, mm), as well as bone strength indicators such as maximum, minimum and polar moments of inertia (I_{max}, I_{min}, and pMOI, mm^4), which describe the shape/distribution of cortical bone (larger values indicate a higher bending strength).

Real-time PCR

Adipose tissues (brown and gonadal) were collected from WT and *Trpm8-KO* mice for RNA extraction under liquid nitrogen conditions. Total RNA was prepared using the standard TRIzol (Sigma-Aldrich) method for tissues. RNA was treated with RNase-Free Recombinant DNAse 1 (Roche) and cDNA was generated using the High Capacity cDNA Reverse Transcriptase Kit (Applied Biosystems) using random primers according to the manufacturer's instructions. mRNA expression analyses was carried out using an iQ SYBR Green Supermix with a BioRad® Laboratories CFX Connect Real-time System thermal cycler and detection system. TATA binding protein 1 (Tbp1) was used as an internal standard control gene for all quantification [22]. Primers used were from Integrated DNA Tecnologies (IDT) (Coralvile, IA) [23–25] and Primer Design (Southampton, UK). All primer sequences are listed in S1 Table. Gene expression values were obtained using the standard double delta Ct method. Samples from WT room temperature mice were set to one by dividing all fold change values from each individual gene by the mean of the WT room temperature fold change values for that gene.

Statistical analysis

GraphPad Prism 8® software was used to visualize data and perform statistical analyses. Data are presented as mean ± standard error. Student's t test or two-way ANOVA was performed with Holm-Sidak *post hoc* multiple comparison test after a significant interaction p-value. $p<0.05$ was considered statistically significant.

Results

Body composition and two-dimensional areal bone density (n = 14-19/group) were assessed at 52 weeks of age in mice housed at standard room temperature (22˚C) (Fig 1). Both male and female *Trpm8-KO* mice had reduced body mass compared to WT mice, which was in part due to a significant reduction in lean mass in males (Fig 1A and 1B) and fat mass in both males and females (Fig 1C and 1D). *Trpm8* deletion suppressed bone mineral density (BMD) and bone mineral content (BMC) (Fig 1E and 1F). In the latter, there was a significant interaction between sex and genotype such that *Trpm8* deletion caused significantly lower bone mineral content in males, but not in females (Fig 1F).

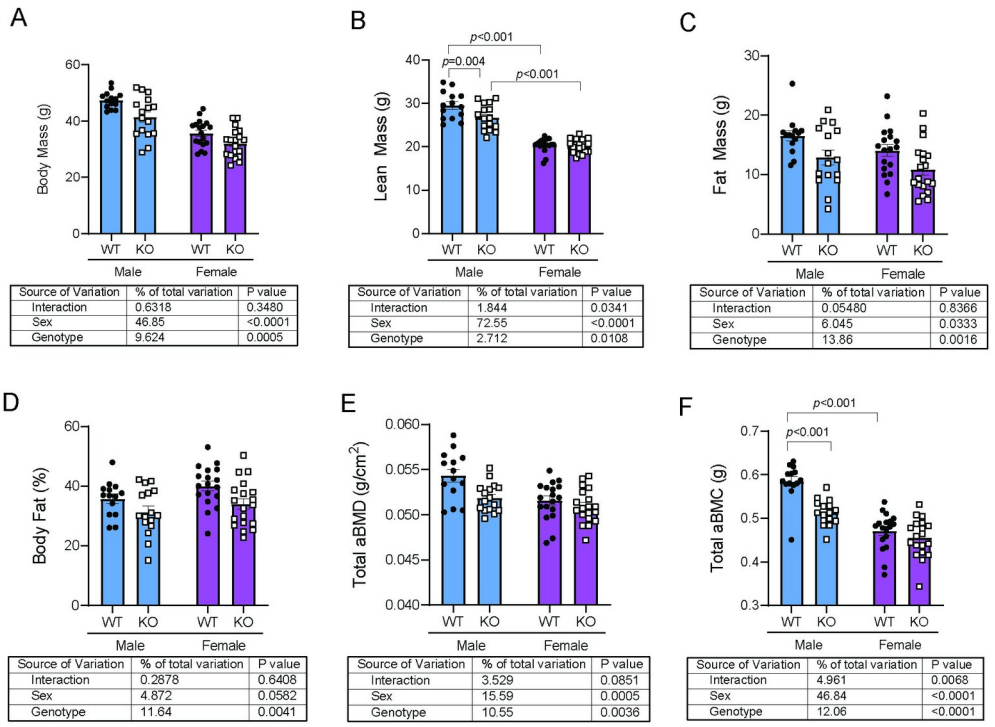

Fig 1. *Trpm8* deletion causes reduced body mass, lean mass and bone density in male mice. (A-D) Body composition in 52-week old male (blue) and female (purple), wildtype (closed circles) and *Trpm8-KO* (open squares) mice was analyzed by DXA. (E, F) Areal total body bone mineral density (aBMD) and areal bone mineral content (BMC) were measured excluding the head. N = 14-19/group. Data are expressed as individual points with bars representing mean ± SEM. Tables below each panel indicate results of the two-way ANOVA, with *p*-values for sex, genotype, and their interaction. *p*-values above the bars represent results from Holm-Sidak *post hoc* test for pairwise significance after a significant interaction effect.

https://doi.org/10.1371/journal.pone.0231060.g001

Because significant changes in two-dimensional DXA data (aBMD and aBMC) are most likely to indicate alterations in cortical microarchitecture, we next examined whether *Trpm8* deletion led to changes in cortical bone by micro Computed Tomography (μCT) (Fig 2). *Trpm8-KO* mice had significantly lower femur total cross-sectional area (total area) and lower marrow area compared to WT mice (Fig 2A–2E). Polar moment of inertia (an indicator of strength), was also dependent upon genotype (p = 0.0479) (Fig 2G). Other parameters, such as cortical tissue mineral density and cortical thickness were not dependent upon genotype (Fig 2F, 2H and 2I). However, femur length was significantly altered by genotype, with *Trpm8-KO* mice having shorter femurs compared to WT (Fig 2J). Finally, to test whether changes in bone density were a result of altered trabecular microarchitecture, we performed μCT on the distal femur (Fig 3). Deletion of *Trpm8* did not influence volumetric trabecular architecture in male or female mice (Fig 3). Taken together, these results indicate smaller bone size in the male *Trpm8-KO* mice may have led to the reduced total body bone mineral content and density.

Previous studies have demonstrated that TRPM8 regulates brown adipose tissue function, and thermogenesis has been associated with changes in trabecular bone remodeling [6, 18, 19]. We next wanted to test, 1) whether a 4-week cold housing challenge would lead to trabecular bone loss and 2) whether TRPM8 was necessary for the adipose tissue and bone responses to cold (Fig 4A). Mice were separated into individual cages and then left at room temperature or moved to 18˚C (Fig 4A). After one week, the temperature was changed from 18˚C to 4˚C. Male *Trpm8-KO* mice had a poorer response to the cold challenge than WT, with core

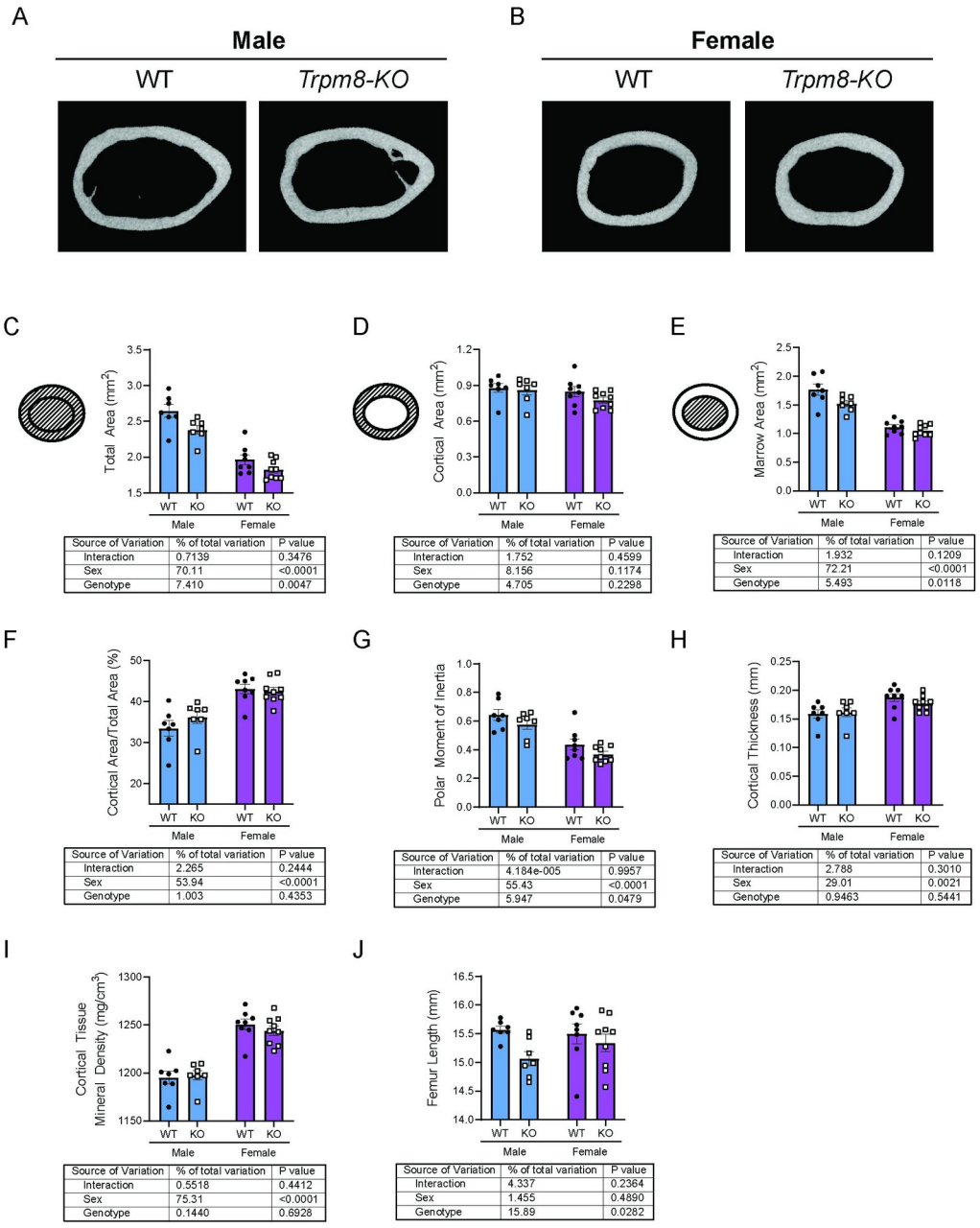

Fig 2. *Trpm8* deletion reduced femur size in male mice. Femurs from room temperature housed male and female *Trpm8-KO* and WT mice were scanned by μCT. (A, B) Representative images of the femur cross section from the midshaft, where cortical microarchitectural measurements were performed (C-J). Cortical bone images were taken of the mouse using the median total area value within each group. Shaded areas of the pictograms in C, D represent the region of interest for each measurement. N = 7–9 per group. Data are expressed as individual points with bars representing mean ± SEM. Tables below each panel indicate results of the two-way ANOVA, with *p*-values for sex, genotype and their interaction. *p*-values above the bars represent results from Holm-Sidak *post hoc* test for pairwise significance after a significant interaction effect.

https://doi.org/10.1371/journal.pone.0231060.g002

temperature being lower in the KO (Fig 4B). Interestingly, the impact of housing temperature change on female mouse core temperature was not dependent upon genotype. By the end of week 2, male *Trpm8-KO* mice had acclimated to the cold exposure and reached core temperatures similar to those of male WT mice (Fig 4C) which was maintained until the endpoint of

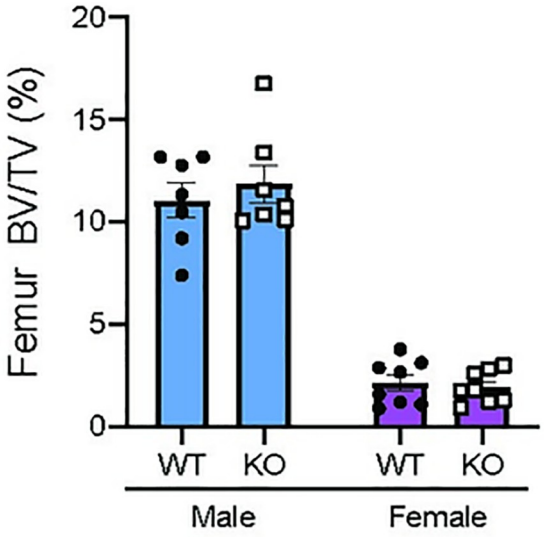

Source of Variation	% of total variation	P value
Interaction	0.2518	0.4360
Sex	89.23	<0.0001
Genotype	0.08133	0.6567

Fig 3. *Trpm8* deletion did not overtly impact trabecular microarchitecture of the distal femur. Bone volume fraction (BV/TV) of the trabecular bone of the distal femur was measured in male and female *Trpm8-KO* and WT mice. N = 7–8 per group. Data are expressed as individual points with bars representing mean ± SEM. Table below the panel indicate results of the two-way ANOVA, with *p*-values for sex, genotype and their interaction. *p*-values above the bars represent results from Holm-Sidak *post hoc* test for pairwise significance after a significant interaction effect.

https://doi.org/10.1371/journal.pone.0231060.g003

the study. Moreover, weight loss was not influenced by *Trpm8* deletion or sex after 4 weeks of the cold challenge (Fig 4D).

Previous studies have shown that impaired BAT function in response to cold was associated with bone loss [26]. Therefore, we next wanted to identify changes in BAT with cold treatment. Cold exposure induced BAT expansion in male WT and *Trpm8-KO* mice (Fig 5A). In contrast, the expansion of BAT mass in female mice was observed only in the WT group ($p = 0.002$) in response to cold, but not in female *Trpm8-KO* mice. In H&E stained sections of BAT, we observed larger lipid droplets in BAT from males of all genotypes and treatments, as well as in female *Trpm8-KO* mice at room temperature. Other female groups had less lipid accumulation, including in the female *Trpm8-KO* mice after cold. We also observed that cold treatment increased *Acadl* and *Ucp1* gene expression in BAT from male mice, and that *Trpm8* deletion elevated *Prdm16*, *Pgc1a*, and *Pparg2* in both housing temperatures. Although the level of *Ucp1* expression was not different betweenWT and *Trpm8-KO* at either temperature, other thermogenic markers (*Cidea* and *Dio2*) were only elevated by cold temperature in the male KO mice (Fig 5C). Changes in BAT gene expression were less striking in females compared to males, with cold treatment inducing *Ucp1* and suppressing *PParg2* and *Prdm16* in both genotypes (Fig 5C). Deletion of *Trpm8* also suppressed *Prdm16*, *Pparg2* and *Pdk4*. However, no significant interaction terms were found in female BAT gene expression. Together, these results indicate *Trpm8* influences the BAT response to temperature change in males and females differently.

Although we did not find any significant differences in inguinal WAT weight (S1 Fig), we did identify that gonadal adipose tissue (gWAT) mass was significantly lowered by cold

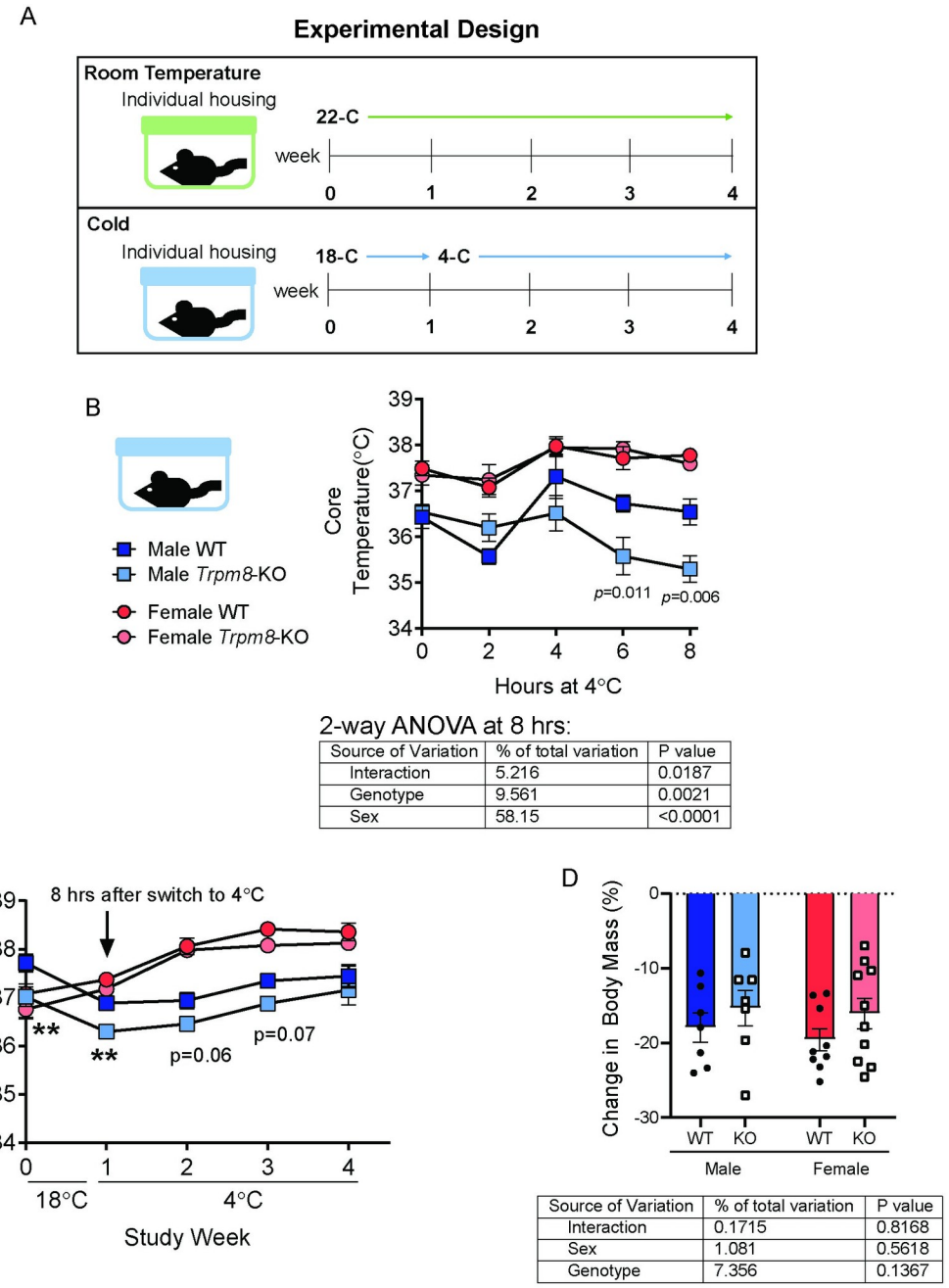

Fig 4. Male *Trpm8-KO* mice had lower core temperature during acclimatization to cold. (A) At 52 weeks of age, mice were separated into individual cages and half were kept at room temperature while the other half were moved to a cold room set at 18˚C. After one week, the temperature was changed to 4˚C and mice were maintained for 3 additional weeks. (B) During the temperature change from 18˚C to 4˚C, core temperature was measured every 2 hours. (C) Weekly core temperature, starting from time zero before mice were moved into the cold, and including the data from the 8 hour time point of the day the temperature changed from 18˚C to 4˚C. (D) Percent change in body weight. N = 7-11/group. Temperature data points represent mean ± SEM. Body weight data are expressed as individual points with bars representing mean ± SEM. Table below panels B and D indicate results of the two-way ANOVA (performed using data from 8 hr time point in B), with *p*-values for sex, genotype and their interaction.

https://doi.org/10.1371/journal.pone.0231060.g004

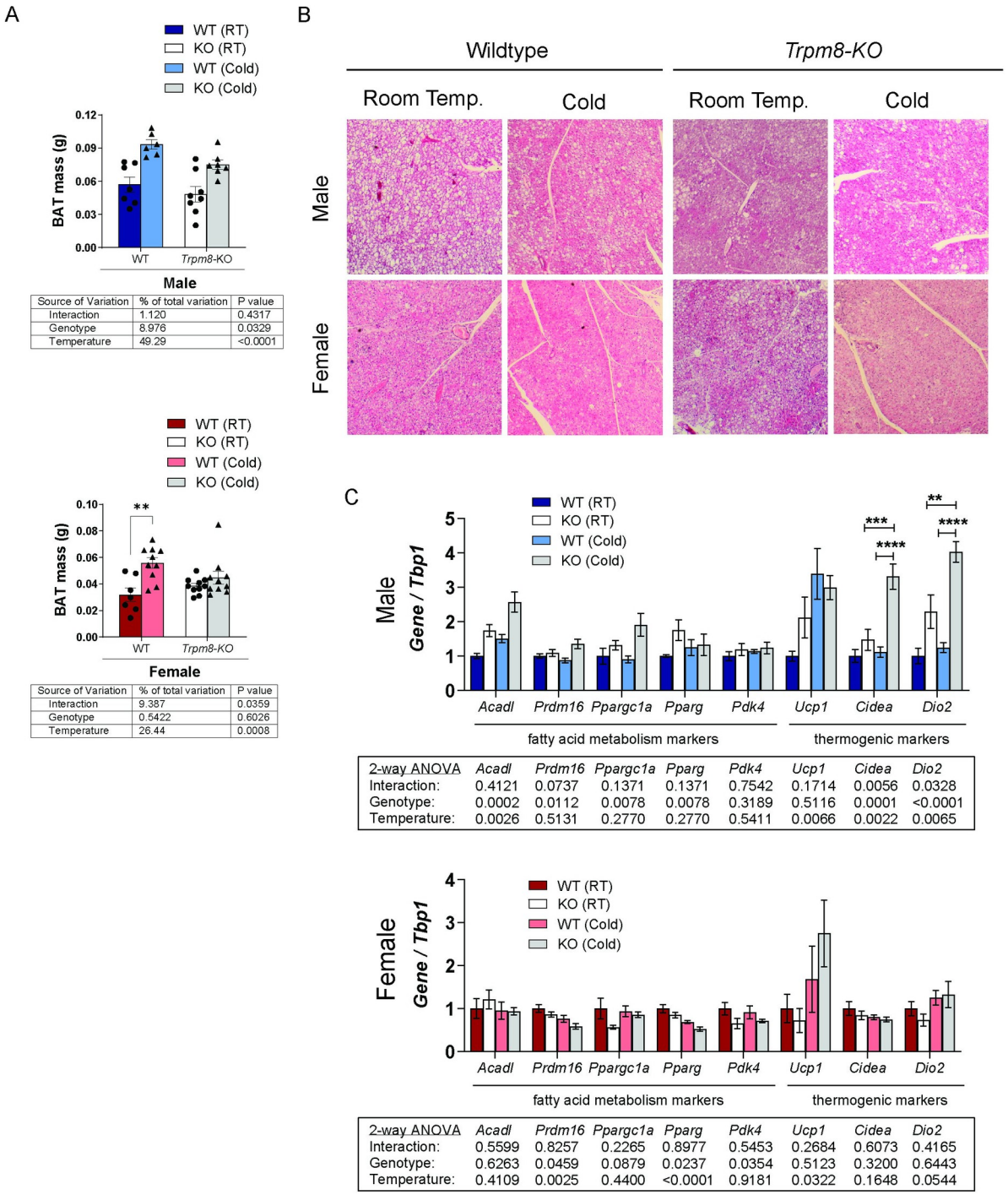

Fig 5. TRPM8 influences the response of BAT to cold temperature. (A) BAT weights from male and female WT and *Trpm8-KO* housed at 22˚C and 4˚C. N = 6–10. (B) Representative H&E stained image of BAT. N = 5–8. (C) Gene expression of fatty acid metabolism and thermogenic markers in male (top) and female (bottom) BAT. N = 5–6. Data presented as mean ± standard error. $^{*}p<0.05$, $^{**}p<0.01$, $^{***}p<0.001$, $^{****}p<0.0001$ by Holm-Sidak *post hoc* test after a significant two-way ANOVA interaction *p*-value.

https://doi.org/10.1371/journal.pone.0231060.g005

housing in both males and females (Fig 6A). H&E staining was suggestive of the presence of beige adipocytes after cold treatment in all sexes and genotypes except the *Trpm8-KO* cold treated males. The development of beige adipocytes was most striking in female *Trpm8-KO*

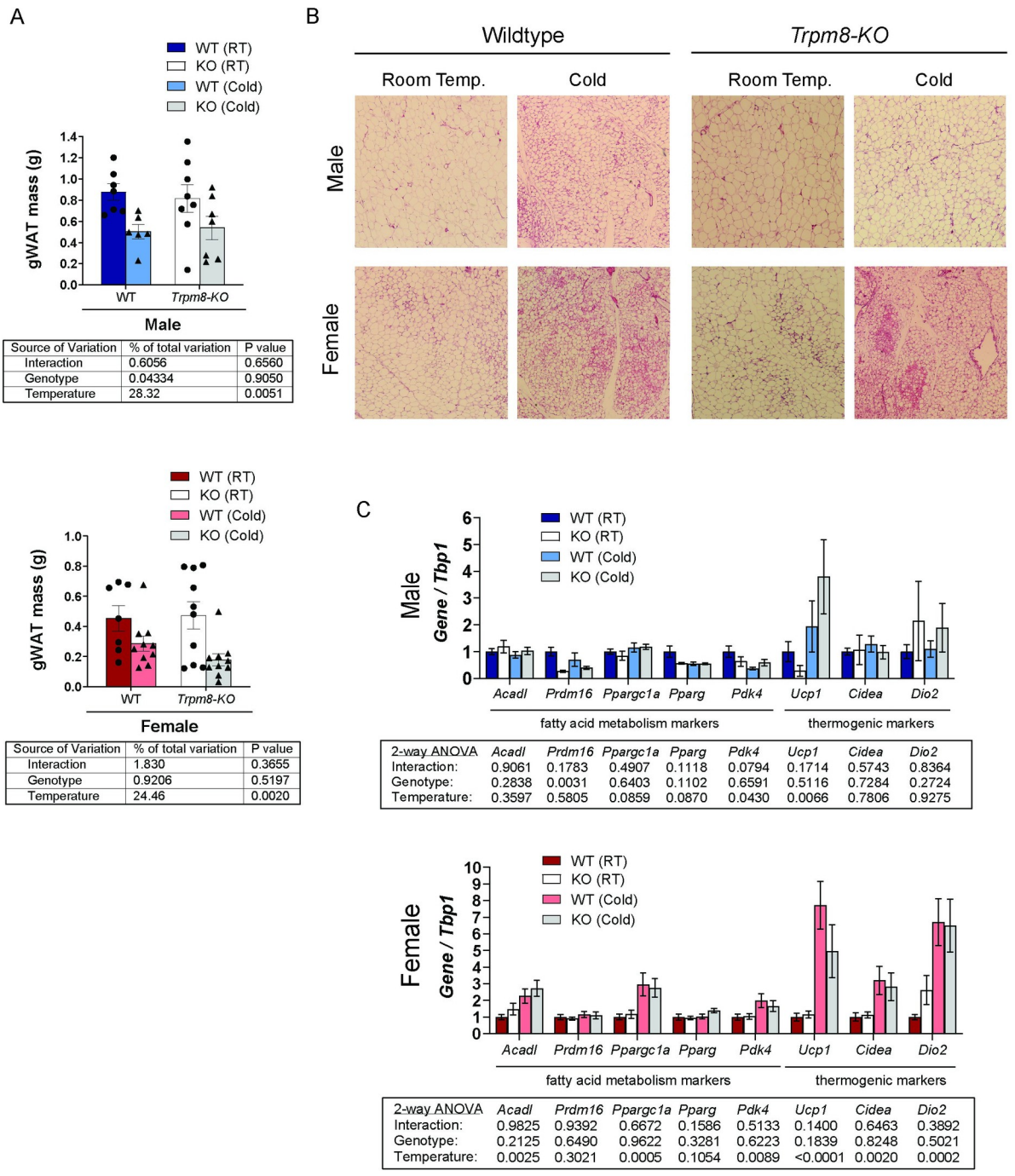

Fig 6. Loss of *Trpm8* prevented beige adipocyte formation in gonadal adipose tissue from male but not female mice. (A) gWAT weights from male and female WT and *Trpm8-KO* housed at 22˚C and 4˚C. N = 6–10. (B) Representative H&E stained image of gWAT. N = 3–7. (C) Gene expression of fatty acid metabolism and thermogenic markers in male (top) and female (bottom) gWAT. N = 4–7. Data presented as mean ± standard error.

https://doi.org/10.1371/journal.pone.0231060.g006

mice, however, suggesting a sex-difference in the way TRPM8 influences gWAT utilization during the acclimatization to cold. These findings were supported by gene expression in gWAT in female mice, which showed, among other things, a 5 to 8-fold increase in *Ucp1* expression after cold, while the male mice only had a 2- and 4-fold increase in WT and KO,

Table 1. Femoral and vertebral bone outcomes assessed by μCT of male wildtype (WT) and *Trpm8-Knockout* (*KO*) mice housed at room temperature or cold.

	Room temperature (22˚C)		Cold (4˚C)		*p*-value		
	WT (N = 7)	KO (N = 7)	WT (N = 6)	KO (N = 7)	genotype	temp	interaction
Distal Femur Trabecular Bone							
BV/TV (%)	11.1 ± 0.8	11.9 ± 0.9	8.9 ± 1.0	9.9 ± 1.1	0.36	**0.04**	0.91
Conn.D (1/mm^3)	43 ± 7	58.5 ± 9.0	31.2 ± 5.8	43.1 ± 7.3	0.07	0.08	0.79
Tb.N (1/mm)	3.0 ± 0.1	3.2 ± 0.1	2.8 ± 0.1	3.0 ± 0.1	0.07	0.06	0.67
Tb.Th (mm)	0.059 ± 0.001	0.061 ± 0.003	0.058 ± 0.002	0.056 ± 0.002	0.95	0.15	0.19
Tb.Sp (mm)	0.323 ± 0.017	0.304 ± 0.007	0.347 ± 0.007	0.321 ± 0.011	0.07	0.09	0.78
Femur Midshaft Cortical Bone							
Ct.Th (mm)	0.159 ± 0.007	0.161 ± 0.008	0.160 ± 0.006	0.154 ± 0.004	0.20	0.67	0.52
Ct.Ar (mm^2)	0.88 ± 0.04	0.86 ± 0.04	0.88 ± 0.03	0.82 ± 0.03	0.26	0.49	0.52
Ct.TMD (mgHA/cm^3)	1195 ± 7	1197 ± 5	1198 ± 8	1192 ± 5	0.73	0.79	0.50
Ma.Ar (mm^2)	1.77 ± 0.10	1.52 ± 0.05	1.74 ± 0.11	1.54 ± 0.06	**0.01**	0.97	0.81
Tt.Ar (mm^2)	2.64 ± 0.09	2.38 ± 0.06	2.62 ± 0.12	2.36 ± 0.07	**0.005**	0.77	0.99
Ct.Ar/Tt.Ar (%)	33.5 ± 1.9	36.2 ± 1.5	33.7 ± 1.4	34.8 ± 0.9	0.21	0.67	0.58
pMOI (mm^4)	0.64 ± 0.04	0.58 ± 0.04	0.64 ± 0.04	0.54 ± 0.03	**0.04**	0.63	0.72
Imax (mm^4)	0.42 ± 0.03	0.40 ± 0.03	0.42 ± 0.03	0.37 ± 0.03	0.19	0.53	0.67
Imin (mm^4)	0.22 ± 0.01	0.18 ± 0.01	0.22 ± 0.02	0.18 ± 0.01	**0.0009**	0.89	0.89
L5 Vertebral Trabecular Bone							
BV/TV (%)	21.6 ± 1.1	20.7 ± 1.8	18.7 ± 0.5	18.4 ± 0.7	0.59	**0.04**	0.78
BS/BV (mm^2/mm^3)	43.9 ± 1.5	44.5 ± 1.9	46.2 ± 0.4	46.9 ± 0.3	0.62	0.08	0.95
BMD (mgHA/cm^3)	226.4 ± 10.0	217.3 ± 16.1	198.2 ± 4.7	197.6 ± 5.9	0.65	**0.03**	0.69
Conn.D (1/mm^3)	127 ± 11	115 ± 8	113 ± 5	119 ± 8	0.73	0.53	0.32
Tb.N (1/mm)	4.4 ± 0.1	4.3 ± 0.1	4.1 ± 0.1	4.2 ± 0.1	0.94	0.11	0.43
Tb.Th (mm)	0.050 ± 0.001	0.053 ± 0.002	0.050 ± 0.003	0.053 ± 0.002	0.10	0.96	0.96
Tb.Sp (mm)	0.215 ± 0.007	0.223 ± 0.009	0.236 ± 0.005	0.230 ± 0.009	0.89	0.08	0.37

Abbreviations: BV/TV, bone volume fraction; Conn.D, connectivity density; Tb.N, trabecular number; Tb.Th, trabecular thickness; Tb.Sp, trabecular separation; Ct.Th, average cortical thickness; Ct.Ar, cortical bone area; Ct.TMD, cortical tissue mineral density; M.Ar, marrow area; T.Ar, total cross-sectional area; Ct.Ar/T.Ar, cortical area fraction; pMOI, polar moment of inertia; Imax, maximum moment of inertia; Imin, minimum moment of inertia; BMD, bone mineral density; BS/BV, specific bone surface.

https://doi.org/10.1371/journal.pone.0231060.t001

respectively, after cold treatment (Fig 6C). Similarly, female mice also had significant increases in *Acadl*, *Pparc1a*, *Pdk4*, *Cidea* and *Dio2* in the cold, whereas males only had a suppression of *Prdm16* in KO, and a suppression of *Pdk4* with cold (Fig 6C). Taken together, these data indicate TRPM8 may be required for beiging of gWAT tissue in males but not females. Further, females may be more prone to generate beige adipocytes in gWAT than males, which could explain their advantage over males in adjusting to cold temperature.

Because altered thermogenesis has previously been associated with changes in bone homeostasis, we next examined bone microarchitectural phenotypes of WT and *Trpm8-KO* mice at room temperature and cold. In addition to cortical bone changes due to genotype and sex noted above in mice at room temperature (Fig 2), we determined that cold temperature caused trabecular bone loss (decreased BV/TV) in male mice of both genotypes, in both the femur and the vertebrae (Table 1). However, cold temperature treatment did not influence cortical bone in either genotype of male mice. In contrast to males, females had only had increased L5 trabecular BS/BV (indicative of trabecular thinning) in response to cold, but no changes in BV/TV in either the femur or the vertebral trabecular bone (Table 2). Medullary area was increased with cold, leading to a reduction in cortical area fraction in females (Table 2).

Table 2. Femoral and vertebral bone outcomes assessed by μCT of female wildtype (WT) and *Trpm8-Knockout* (*KO*) mice housed at room temperature or cold.

	Room temperature (22˚C)		Cold (4˚C)		*p*-value		
	WT (N = 8)	KO (N = 8–9)	WT (N = 8–9)	KO (N = 8–11)	genotype	temp	interaction
Distal Femur Trabecular Bone							
BV/TV (%)	2.13 ± 0.38	2.78 ± 0.90	1.87 ± 0.20	2.58 ± 0.78	0.32	0.73	0.97
Conn.D (1/mm^3)	4.3 ± 1.4	14.4 ± 7.9	6.6 ± 1.7	15.9 ± 10.7	0.21	0.81	0.96
Tb.N (1/mm)	1.7 ± 0.1	1.8 ± 0.1	1.7 ± 0.1	1.8 ± 0.1	0.46	0.74	0.62
Tb.Th (mm)	0.060 ± 0.003	0.056 ± 0.003	0.052 ± 0.001	0.054 ± 0.003	0.56	0.07	0.27
Tb.Sp (mm)	0.611 ± 0.039	0.584 ± 0.037	0.588 ± 0.027	0.585 ± 0.32	0.67	0.74	0.72
Femur Midshaft Cortical Bone							
Ct.Th (mm)	0.188 ± 0.007	0.177 ± 0.004	0.177 ± 0.004	0.174 ± 0.004	0.16	0.16	0.42
Ct.Ar (mm^2)	0.85 ± 0.04	0.78 ± 0.02	0.82 ± 0.02	0.78 ± 0.02	**0.04**	0.71	0.62
Ct.TMD (mgHA/cm^3)	1251 ± 6	1244 ± 5	1248 ± 5	1241 ± 4	0.16	0.55	0.93
Ma.Ar (mm^2)	1.12 ± 0.04	1.05 ± 0.03	1.21 ± 0.05	1.14 ± 0.03	0.08	**0.02**	0.89
Tt.Ar (mm^2)	1.97 ± 0.07	1.83 ± 0.04	2.03 ± 0.06	1.92 ± 0.04	**0.02**	0.14	0.81
Ct.Ar/Tt.Ar (%)	43.1 ± 1.2	42.6 ± 1.0	40.7 ± 0.9	40.7 ± 0.8	0.80	**0.03**	0.76
pMOI (mm^4)	0.44 ± 0.04	0.37 ± 0.02	0.44 ± 0.02	0.37 ± 0.03	**0.02**	0.91	0.98
Imax (mm^4)	0.29 ± 0.03	0.24 ± 0.01	0.28 ± 0.02	0.25 ± 0.01	**0.02**	0.80	0.78
Imin (mm^4)	0.15 ± 0.01	0.13 ± 0.01	0.16 ± 0.01	0.15 ± 0.01	0.05	0.33	0.65
L5 Vertebral Trabecular Bone							
BV/TV (%)	15.8 ± 1.2	13.1 ± 0.5	14.2 ± 1.2	12.0 ± 0.5	**0.01**	0.16	0.81
BS/BV (mm^2/mm^3)	38.2 ± 1.3	40.9 ± 1.1	41.5 ± 1.2	43.4 ± 1.7	0.10	**0.04**	0.77
BMD (mgHA/cm^3)	174 ± 12	148 ± 4	158 ± 12	138 ± 4	**0.02**	0.15	0.80
Conn.D (1/mm^3)	51 ± 9	48 ± 7	60. ± 7	48 ± 8	0.36	0.55	0.57
Tb.N (1/mm)	2.67 ± 0.07	2.43 ± 0.12	2.68 ± 0.11	2.44 ± 0.09	**0.02**	0.90	0.99
Tb.Th (mm)	0.061 ± 0.002	0.057 ± 0.002	0.056 ± 0.001	0.054 ± 0.002	0.15	0.06	0.64
Tb.Sp (mm)	0.382 ± 0.009	0.428 ± 0.024	0.384 ± 0.014	0.423 ± 0.016	**0.02**	0.90	0.83

Abbreviations: BV/TV, bone volume fraction; Conn.D, connectivity density; Tb.N, trabecular number; Tb.Th, trabecular thickness; Tb.Sp, trabecular separation; Ct.Th, average cortical thickness; Ct.Ar, cortical bone area; Ct.TMD, cortical tissue mineral density; M.Ar, marrow area; T.Ar, total cross-sectional area; Ct.Ar/T.Ar, cortical area fraction; pMOI, polar moment of inertia; Imax, maximum moment of inertia; Imin, minimum moment of inertia; BMD, bone mineral density; BS/BV, specific bone surface.

https://doi.org/10.1371/journal.pone.0231060.t002

However, there were no significant temperature by genotype interactions in trabecular or cortical bone parameters in either sex, suggesting bone loss from cold was not dependent upon TRPM8 in males or females (Tables 1 and 2). Of note, female but not male mice had reduced vertebral BV/TV, BMD, Tb.N. and increased Tb.Sp when *Trpm8* was absent (Table 2), but these parameters did not significantly change with housing temperature.

Finally, we also evaluated whether cold housing and/or loss of *Trpm8* would affect the adiposity of the bone marrow (Fig 7). In general, BMAT is limited in male mice compared to females (Fig 7A and 7B). In male mice, we did not find any significant effect of either genotype or temperature on marrow adipocyte numbers (Fig 7B). In female mice, there was a significant effect of *Trpm8* deletion on adipocyte number (Fig 7B), but there was no effect of housing temperature on BMAT in females.

Discussion

In this study, we determined that the impact of *Trpm8* deletion on bone, body temperature and adipose tissue was dependent upon sex and housing temperature (Table 3 summary). Our original hypothesis was that *Trpm8* deletion would impair body temperature regulation, but

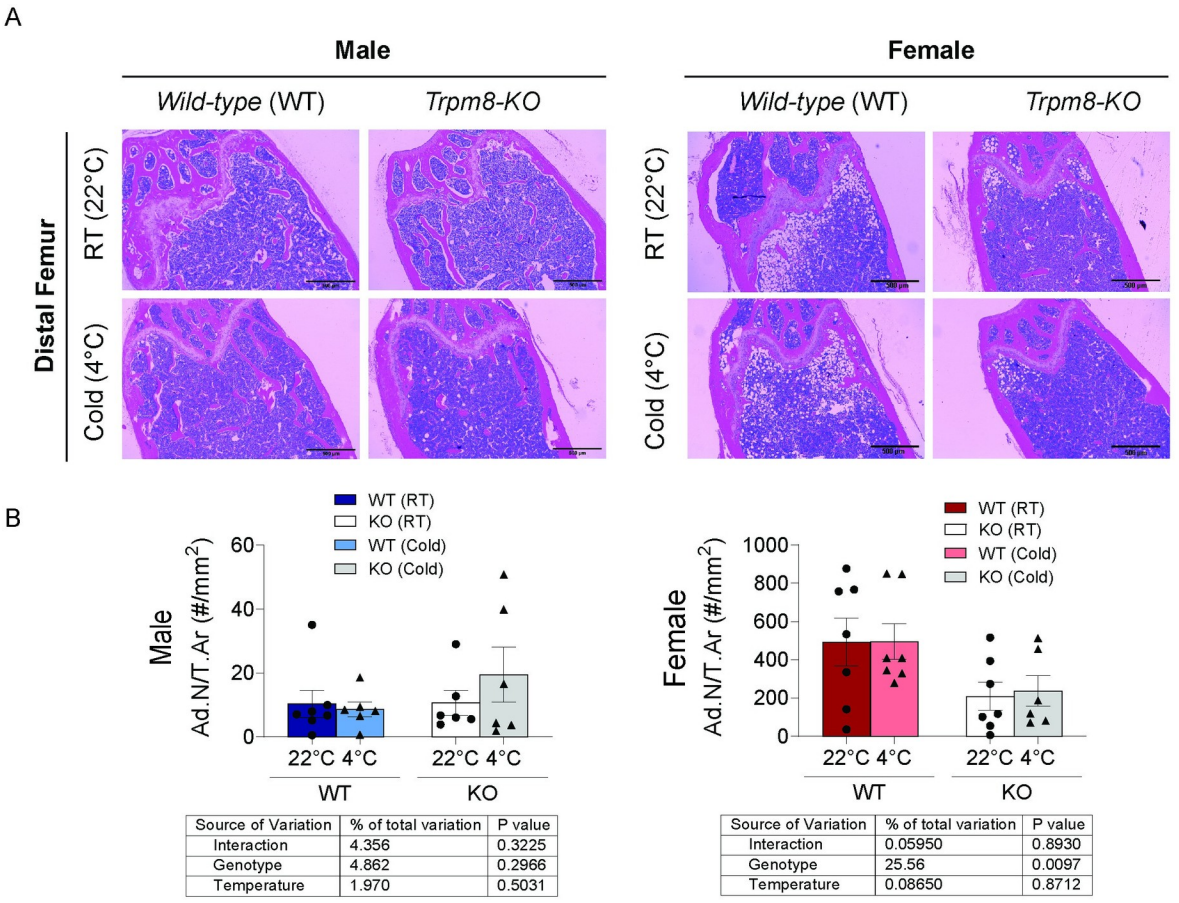

Source of Variation	% of total variation	P value
Interaction	4.356	0.3225
Genotype	4.862	0.2966
Temperature	1.970	0.5031

Source of Variation	% of total variation	P value
Interaction	0.05950	0.8930
Genotype	25.56	0.0097
Temperature	0.08650	0.8712

Fig 7. *Trpm8* deletion suppressed marrow adipose tissue in female mice. (A) Representative histological images of the distal femur metaphysis from male and female WT and *Trpm8-KO* mice housed at standard room temperature (RT) (22˚C) and cold temperature (4˚C). Scale bar = 500 μm. (B) Quantification of adipocyte numbers (Ad.N) corrected for total area (T.Ar). N = 7/group. Data presented as mean ± standard error.

https://doi.org/10.1371/journal.pone.0231060.g007

would also protect against cold-induced changes in bone and marrow adipose tissue. Males, but not females, had impaired temperature regulation after *Trpm8* deletion. However, cold housing led to trabecular bone loss in males and cortical bone loss in females, independent of genotype, which is consistent with previous studies showing that cold housing can negatively impact the skeleton [1, 6]. It has also previously been shown that cold housing is associated with reduced BMAT [27]. However, our findings indicate that in females BMAT was highly dependent upon *Trpm8* but not dependent upon housing temperature, pointing toward potentially diverse function of TRPM8 in regulating BMAT levels as well as bone. Despite the

Table 3. Summary of results.

	Males		Females	
	***Trpm8* Deletion**	**Cold Housing**	***Trpm8* Deletion**	**Cold Housing**
Body Temperature	Sex by genotype interaction–temperature reduced in male KOs but not female KOs in cold			
Cortical Bone	Decreased cross-sectional area	Unchanged	Decreased cross-sectional area	Decreased medullary area
Trabecular Bone	Unchanged	Decreased	Decreased (vertebrae only)	Increased BS/BV (trend toward decreased bone)
Marrow Adiposity	Unchanged	Unchanged	Decreased	Unchanged

https://doi.org/10.1371/journal.pone.0231060.t003

lack of any temperature by genotype interaction effects on bone parameters, it is worth noting that male KO mice, with impaired temperature regulation, tended to have a more striking difference in bone size. Furthermore, female KO mice had significant trabecular bone loss in the vertebrae but not the femur, indicating potential site-specific effects of *Trpm8* deletion on bone. Until now, a bone phenotype in *Trpm8-KO* mice has not been previously described.

Recently, Iwaniec et al. (2016) highlighted that the current standard room temperature housing (22˚C) can already be considered a cold environment to mice and that it was associated with bone loss in growing females compared to thermoneutral housing [1]. A *Trpm8* functional cold circuit is established after birth around postnatal day 14 [28]. Others have found that *Trpm8* is a regulator of energy metabolism and thermogenesis [12, 15, 17], and our findings are consistent with the latter, showing that its deletion can cause a difference in the expression of thermogenic markers, particularly in male BAT, and lower body weight at room temperature. This suggests that the absence of *Trpm8* during the developmental phase might be associated with defective cold circuits which partially fail to sustain optimal body temperature, as previously described [12]. However, the way temperature regulation is related to bone in this context is unclear, and the mechanism of low bone mass in *Trpm8-KO* mice will need to be determined in future work. Some *in vitro* evidence suggests human osteoblast-like cells and murine osteoblast cells express *Trpm8*, but the functional role in bone *in vivo* is unclear [29, 30]. Although the deletion of other *Trp* channels, such as *Trpv1* [31] and *Trpv5* [32], has been reported to induce bone loss in animal models, there is a lack of data exploring the physiological role of TRPM8 in skeletal homeostasis.

One interesting finding was that *Trpm8* deletion in females caused decreased BMAT content. Aging generally leads to accumulation of bone marrow adipose tissue in the distal femur and proximal tibia in mice, but the mechanisms and consequences of this accumulation remain an area of active investigation. Both osteoblasts and adipocytes arise from a shared mesenchymal precursor, thus one hypothesis is that situations of bone loss may lead to marrow adiposity by shunting cells away from the osteoblast lineage to the adipocyte lineage (as in calorie restriction, PPARγ2 inhibition, and aging) [33]. However, the alternate, shifting from marrow adipose lineage to osteoblast lineage, does not seem likely in female *Trpm8-KO* mice, since they had indices of reduced bone density in concert with low marrow adiposity. In other situations, like bone loss from the atypical antipsychotic drug risperidone, elevated SNS activity leads to a reduction in both osteoblast-mediated bone formation and marrow adiposity due to inhibitory effects on both lineages [19]. Recently, Wee et al., (2019) elegantly demonstrated that iWAT and BMAT shared sympathetic innervation using retroviral nerve tracing [34]. They revealed that leptin-responsive regions such as paraventricular hypothalamus, arcuate nucleus, dorsomedial hypothalamus, ventromedial hypothalamus, and area postrema were labelled after viral tracing from iWAT, bone marrow, and BMAT [34]. However, it remains unclear if sex-differences exist in neural regulation of these tissues, and if gWAT would be regulated by similar common sympathetic pathways. Whether elevated SNS activity to stimulate thermogenesis could be responsible for bone loss and reduced marrow adiposity with *Trpm8* deletion in room temperature mice would be an interesting avenue for further research.

Investigations into sex differences in the thermogenic response to *Trpm8* deletion have been limited. Clearly, *Trpm8* is important for the detection of environmental cooling [10, 11, 35] and it has also been implicated in BAT thermogenesis and thermoregulatory processes [12, 17, 18]. Early publications on *Trpm8* had reported no differences in core temperature associated with its global deletion in mice [35]. Ma et al. (2012) demonstrated that menthol activates UCP-1 dependent thermogenesis and increases core temperature in WT mice, but that when TRPM8 is deleted, this activation is absent [18]. In contrast, our studies use cold-temperature to induce thermogenesis, and show a partial dependence on TRPM8. However, our findings

also indicate that other pathways may compensate for the loss of TRPM8, especially in the females. Specifically, *Trpm8-KO* male mice struggled to increase body temperature to the level of WT in a cold environment (of which, menthol treatment is partly mimicking). However, the study by Ma, et al. (2012) did not directly compare WT to KO body temperature, so it is difficult to align perfectly with our findings. Recently, Reimúndez et al. (2018) demonstrated that *Trpm8* is required for thermoregulation in male mice when housed in colder environments, which corroborates our findings [12]. Interestingly, Reimúndez et al. (2018) also demonstrated that this difficulty in maintaining core temperature was associated with greater tail vasodilation and heat loss in male mice with global deletion of *Trpm8*, indicating that this cold-sensing channel has an important role in regulating both thermogenesis and heat dissipation [12]. However, female core temperature status was not investigated in any of these studies.

In contrast, one strength of our study is the comprehensive analyses of mice of both sexes. Cooling sensitivity is the first step to activate the cold response neuronal mechanism that modulates lipolysis and energy expenditure [36]. In our study, we observed that cold-induced weight loss occurred in both sexes, irrespective of the genotype. However, there were *Trpm8*- and sex-differences among the various adipose tissues' response to housing temperature. Male mice housed at 4˚C exhibited BAT expansion with fewer lipid droplets and increased *Ucp1* expression in WT, which is indicative of thermogenesis activity. However, this difference did appear to be blunted in KO mice (Fig 5). Moraes et al. (2017) found reduced *Ucp1* and *Pparg* expression at zeitgeber time (ZT, where ZT0 = onset of lights on) ZT2 and ZT14 in male TRPM8-KO mice ranging from 3–6 months of age, compared to ours that were 12 months [16]. Although we did not see lower *Ucp1* or *Pparg* in our room temperature mice, we expect that this difference might be due to the age of the mice or the time of the day that our tissues were collected ZT6-ZT10. However, our overall finding that thermogenesis is impaired in males KO mice is consistent with Moraes et al. finding of reduced *Ucp1* [16]. Further, we found that cold housing in male KO, but not WT, mice induced a robust expression of other thermogenic markers such as *Cidea* and *Dio2* in BAT, which may have been compensatory for any impairment in BAT function.

In females, we found that cold housing led to an increase in *Ucp1* expression and reduction in lipid droplets in BAT, and TRPM8 was not required for the response. However, TRPM8 was required for BAT expansion in response to cold, as well as normal expression of several fatty acid metabolism markers in BAT. Furthermore, cold reduced gWAT mass in female mice from both genotypes, in addition to increasing expression of fatty acid metabolism (*Acadl*, *Pgc1α*, *Pdk4*) and thermogenic (*Ucp1*, *Cidea*, *Dio2*) markers. It should be considered that estrogen status may play a role in sex-differences in thermogenesis and WAT beiging found in the present study. Several studies observed that the beiging process does take place in gWAT in females [37, 38]. Increased expression of beiging markers such as *Ucp1*, *Pgc1α*, *Elovl3*, *Cidea* was observed in gWAT after either 10 days of cold exposure [38] or β3-adrenergic receptor agonist treatment [37] in female mice. Kim et al. (2016) demonstrated that gWAT in females is more susceptible to the beiging process than in males, due to more extensive sympathetic innervation inducing brown adipogenesis [37]. Also, the authors showed that sympathetic innervation of gWAT is sex-hormone dependent, as reduced tyrosine hydroxylase protein levels and lack of beiging of gWAT was found after chemical ovarian ablation [37]. Indeed, lipolysis can be directly modulated by estrogen through estrogen receptor alpha (ERα) signaling in BAT and WAT adipocytes [39]. Estrogen also has been described to play a critical role in cold sensitivity and hyperalgesia [40, 41], which are also functions thought to be regulated by *Trpm8* [42, 43]. However, interestingly, a previous preclinical study observed that *Trpm8* expression was upregulated in the skin of ovariectomized rats compared to sham control rats

[44] and β-estradiol treatment might reduce *Trpm8* overexpression in the skin of ovariectomized rats [45]. These findings support our data that suggest regulation of energy metabolism in female mice is independent of *Trpm8* cold-sensing function and estrogen might be a more relevant factor to normal thermoregulation in females. It is unclear however, whether ovariectomized mice, or mice aged to natural amenorrhea, would have a response to cold that is modified by *Trpm8* deletion.

The global deletion of *Trpm8* may have led to compensatory changes in other thermogenic mechanisms, which may have been sex-dependent. In addition to TRPM8, there is another cold-activated *Trp* channel known as transient receptor potential ankyrin 1 (TRPA1) which is considered to be a noxious cold receptor [46]. Interestingly, TRPM8 and TRPA1 appear to function in both complementary and synergistic fashion to detect environmental innocuous and noxious cold [46]. Winter et al. (2017) found that the lack of *Trpm8* and *Trpa1* led to a striking reduction in cold avoidance behavior in mice [46]. However, an acute cold avoidance response was still observed in *Trpm8-KO* mice with functional TRPA1 when exposed to a temperature range between 28˚C and 15˚C [46]. This suggests that TRPA1 can only partially compensate for the absence of TRPM8 [46]. When cold-defense mechanisms, such as thermogenesis and vascular tone, fail to sustain an optimal body temperature, a shivering response is triggered to increase heat generation [47]. In our study, only occasional shivering-like behaviors were observed in some mice. These resolved quickly and we did not note any differences in the genotypes of the mice that shivered. Previous studies found that *Trpm8* is not required to induce shivering and tachycardia during cold challenge [47]. Instead, shivering is found to be regulated by TRPV1 [47], which once more indicates TRPM8 is a major regulator of non-shivering thermogenesis.

In summary, our findings support that *Trpm8* is important for body temperature maintenance in male mice and its absence triggers a compensatory response to counteract reduction in core temperature. Moreover, *Trpm8* does not appear to regulate the bone response to colder environments, where the sympathetic nervous system-mediated stress response and/or diversion of energy away from bone may be important in contributing to bone loss. Interestingly, deletion of *Trpm8* was associated with bone size and shape differences, which tended to be more striking in males. Therefore, although any bone loss associated with cold housing may be independent of TRPM8, low bone mass found in *Trpm8*-KO mice compared to WT, indicates that the functions of TRPM8 could contribute to bone modeling and remodeling throughout lifespan.

Limitations

Some limitations of this study do exist. First, addition of a thermoneutral group would potentially exacerbate differences observed, and could provide additional insight into whether *Trpm8* regulates bone and marrow adiposity independent of cold temperature sensation and subsequent physiologic response. We regret that we did not have the capability to age mice to 52 weeks of age in a thermoneutral (~28-30˚C) rodent incubator when this study was first designed. Next, because the room temperature mice were housed in a separate room from the cold-treated, we cannot exclude the possibility that the additional noise of the cold room contributed to the phenotype. There is no known association between noise stress and changes in brown adipose tissue, but there are some studies examining the impact of chronic mild stress (CMS), of which one of the stressors is noise, on bone density. One study found that the CMS caused bone loss, and this could be blocked by propranolol, which suggests the SNS is involved [48]. However, other stressors were involved in that study, including water deprivation, continuous overnight illumination, stroboscopic illumination, cage tilt, and time in a soiled cage.

Thus, it is unclear whether noise alone would have influenced bone microarchitecture. Although the sound was greater in the cold room in our study, it was consistent over time, and the fact remains that compared to WT males, and females of both genotypes all treated in the cold, the body temperature in the male KO mice had a delayed response to cold. Other key findings, like *Trpm8-KO* mediated bone loss and reduced marrow adiposity, were not dependent upon housing conditions. Furthermore, additional N would have helped to reduce biological variability, which was high in some of the secondary outcomes of interest, such as inguinal WAT mass and expression of *Ucp1* in both BAT and gWAT. Although differences were not detected in iWAT mass, it is possible that histology and mRNA analyses of this tissue would have provided additional valuable information. However, iWAT samples were not saved to analyze at a later time point. Additionally, examining the thermogenic response at the time point where we observed major differences in body temperature in male mice exposed to cold would have provided better insight into mechanism. However, analysis of bone defects after cold were the primary outcomes of interest, and these would not have been apparent at such an early time point.

Despite these limitations, the current data provide new insight into our understanding of the role of *Trpm8* in the regulation of skeletal homeostasis and thermogenesis, and demonstrate important and unexpected sex-differences in these processes. This work suggests that in males in particular, TRPM8 is necessary for normal thermoregulation and bone density, while in females, TRPM8 regulates marrow adiposity.

Supporting information

S1 Fig. Inguinal WAT weights from male and female WT and *Trpm8-KO* housed at 22˚C and 4˚C. N = 6–10.
(TIF)

S1 Table. qPCR primer information.
(DOCX)

S1 File.
(XLSX)

Acknowledgments

The authors thank Phuong Le and Casey Doucette for the assistance during the cold housing experiment and Audrey Bergeron for critical review of the manuscript. This work utilized services of the following MMCRI cores: the Molecular Phenotyping Core, the Physiology Core, the Histopathology and Histomorphometry Core, and the Mouse Transgenic and In Vivo Imaging Core.

Author Contributions

Conceptualization: Katherine J. Motyl.

Data curation: Adriana Lelis Carvalho, Annika Treyball, Daniel J. Brooks, Samantha Costa, Ryan J. Neilson, Katherine J. Motyl.

Formal analysis: Adriana Lelis Carvalho, Annika Treyball, Daniel J. Brooks, Samantha Costa, Ryan J. Neilson, Katherine J. Motyl.

Funding acquisition: Katherine J. Motyl.

Investigation: Adriana Lelis Carvalho, Annika Treyball, Daniel J. Brooks, Samantha Costa, Ryan J. Neilson, Katherine J. Motyl.

Methodology: Katherine J. Motyl.

Project administration: Katherine J. Motyl.

Resources: Katherine J. Motyl.

Supervision: Katherine J. Motyl.

Validation: Katherine J. Motyl.

Visualization: Adriana Lelis Carvalho, Annika Treyball, Ryan J. Neilson, Katherine J. Motyl.

Writing – original draft: Adriana Lelis Carvalho, Katherine J. Motyl.

Writing – review & editing: Adriana Lelis Carvalho, Annika Treyball, Daniel J. Brooks, Samantha Costa, Ryan J. Neilson, Michaela R. Reagan, Mary L. Bouxsein, Katherine J. Motyl.

References

1. Iwaniec UT, Philbrick KA, Wong CP, Gordon JL, Kahler-Quesada AM, Olson DA, et al. Room temperature housing results in premature cancellous bone loss in growing female mice: implications for the mouse as a preclinical model for age-related bone loss. Osteoporos Int. 2016; 27: 3091–3101. https://doi.org/10.1007/s00198-016-3634-3 PMID: 27189604
2. Fedorenko A, Lishko P V., Kirichok Y. Mechanism of fatty-acid-dependent UCP1 uncoupling in brown fat mitochondria. Cell. 2012; 151: 400–413. https://doi.org/10.1016/j.cell.2012.09.010 PMID: 23063128
3. Tan CL, Knight ZA. Regulation of Body Temperature by the Nervous System. Neuron. 2018; 98: 31–48. https://doi.org/10.1016/j.neuron.2018.02.022 PMID: 29621489
4. Contreras GA, Lee YH, Mottillo EP, Granneman JG. Inducible brown adipocytes in subcutaneous inguinal white fat: The role of continuous sympathetic stimulation. Am J Physiol—Endocrinol Metab. 2014; 307: E793–E799. https://doi.org/10.1152/ajpendo.00033.2014 PMID: 25184993
5. Elefteriou F. Neuronal signaling and the regulation of bone remodeling. Cell Mol Life Sci. 2005; 62: 2339–2349. https://doi.org/10.1007/s00018-005-5175-3 PMID: 16132233
6. Motyl KJ, Bishop KA, Demambro VE, Bornstein SA, Le P, Kawai M, et al. Altered thermogenesis and impaired bone remodeling in Misty mice. J Bone Miner Res. 2013; 28: 1885–1897. https://doi.org/10.1002/jbmr.1943 PMID: 23553822
7. Scheller EL, Doucette CR, Learman BS, Cawthorn WP, Khandaker S, Schell B, et al. Region-specific variation in the properties of skeletal adipocytes reveals regulated and constitutive marrow adipose tissues. Nat Commun. 2015; 6: 7808. https://doi.org/10.1038/ncomms8808 PMID: 26245716
8. Martin SA, Philbrick KA, Wong CP, Olson DA, Branscum AJ, Jump DB, et al. Thermoneutral housing attenuates premature cancellous bone loss in male C57bl/6J mice. Endocr Connect. 2019. https://doi.org/10.1530/EC-19-0359 PMID: 31590144
9. Turner RT, Philbrick KA, Wong CP, Gamboa AR, Branscum AJ, Iwaniec UT. Effects of Propranolol on Bone, White Adipose Tissue, and Bone Marrow Adipose Tissue in Mice Housed at Room Temperature or Thermoneutral Temperature. Front Endocrinol (Lausanne). 2020. https://doi.org/10.3389/fendo.2020.00117 PMID: 32256446
10. Dhaka A, Murray AN, Mathur J, Earley TJ, Petrus MJ, Patapoutian A. TRPM8 Is Required for Cold Sensation in Mice. Neuron. 2007; 54: 371–378. https://doi.org/10.1016/j.neuron.2007.02.024 PMID: 17481391
11. McKemy DD, Neuhausser WM, Julius D. Identification of a cold receptor reveals a general role for TRP channels in thermosensation. Nature. 2002; 416: 52–58. https://doi.org/10.1038/nature719 PMID: 11882888
12. Reimúndez A, Fernández-Peña C, García G, Fernández R, Ordás P, Gallego R, et al. Deletion of the cold thermoreceptor TRPM8 increases heat loss and food intake leading to reduced body temperature and obesity in mice. J Neurosci. 2018; 38: 3643–3656. https://doi.org/10.1523/JNEUROSCI.3002-17.2018 PMID: 29530988

13. Zhu Z, Ma S, Yu H, Zhao Z, Luo Z, Chen J, et al. Activation of the cold-sensing TRPM8 channel triggers UCP1-dependent thermogenesis and prevents obesity. J Mol Cell Biol. 2012; 4: 88–96. https://doi.org/10.1093/jmcb/mjs001 PMID: 22241835

14. McCoy DD, Zhou L, Nguyen AK, Watts AG, Donovan CM, McKemy DD. Enhanced insulin clearance in mice lacking TRPM8 channels. Am J Physiol—Endocrinol Metab. 2013; 305: 78–88. https://doi.org/10.1152/ajpendo.00542.2012 PMID: 23651844

15. Rossato M, Granzotto M, Macchi V, Porzionato A, Petrelli L, Calcagno A, et al. Human white adipocytes express the cold receptor TRPM8 which activation induces UCP1 expression, mitochondrial activation and heat production. Mol Cell Endocrinol. 2014; 383: 137–146. https://doi.org/10.1016/j.mce.2013.12.005 PMID: 24342393

16. Moraes MN, de Assis LVM, Henriques F dos S, Batista ML, Güler AD, Castrucci AM de L. Cold-sensing TRPM8 channel participates in circadian control of the brown adipose tissue. Biochim Biophys Acta—Mol Cell Res. 2017; 1864: 2415–2427. https://doi.org/10.1016/j.bbamcr.2017.09.011 PMID: 28943398

17. Jiang C, Zhai M, Yan D, Li D, Li C, Zhang Y, et al. Dietary menthol-induced TRPM8 activation enhances WAT 1C "browning 1D" and ameliorates diet-induced obesity. Oncotarget. 2017; 8: 75114–75126. https://doi.org/10.18632/oncotarget.20540 PMID: 29088850

18. Ma S, Yu H, Zhao Z, Luo Z, Chen J, Ni Y, et al. Activation of the cold-sensing TRPM8 channel triggers UCP1-dependent thermogenesis and prevents obesity. J Mol Cell Biol. 2012; 4: 88–96. https://doi.org/10.1093/jmcb/mjs001 PMID: 22241835

19. Motyl KJ, DeMambro VE, Barlow D, Olshan D, Nagano K, Baron R, et al. Propranolol attenuates risperidone-induced trabecular bone loss in female mice. Endocrinology. 2015; 156: 2374–2383. https://doi.org/10.1210/en.2015-1099 PMID: 25853667

20. Fischer AW, Cannon B, Nedergaard J. Optimal housing temperatures for mice to mimic the thermal environment of humans: An experimental study. Mol Metab. 2018. https://doi.org/10.1016/j.molmet.2017.10.009 PMID: 29122558

21. Bouxsein ML, Boyd SK, Christiansen BA, Guldberg RE, Jepsen KJ, Müller R. Guidelines for assessment of bone microstructure in rodents using micro-computed tomography. J Bone Miner Res. 2010; 25: 1468–1486. https://doi.org/10.1002/jbmr.141 PMID: 20533309

22. Vengellur A, LaPres JJ. The role of hypoxia inducible factor 1α in cobalt chloride induced cell death in mouse embryonic fibroblasts. Toxicol Sci. 2004. https://doi.org/10.1093/toxsci/kfh278 PMID: 15375294

23. Seale et al. PRDM16 Controls a Brown Fat/Skeletal Muscle Switch. Bone. 2008; 23: 1–7. https://doi.org/10.1038/nature07182 PMID: 18719582

24. Sanchez-Gurmaches; Guertin D. Adipocytes arise from multiple lineages that are heterogeneously and dynamically distributed Access. Nat Commun. 2014; 5: 4099. https://doi.org/10.1038/ncomms5099 PMID: 24942009

25. Cooper MP, Uldry M, Kajimura S, Arany Z, Spiegelman BM. Modulation of PGC-1 coactivator pathways in brown fat differentiation through LRP130. J Biol Chem. 2008. https://doi.org/10.1074/jbc.M805431200 PMID: 18728005

26. Motyl KJ, Bishop KA, Demambro VE, Bornstein SA, Le P, Kawai M, et al. Altered thermogenesis and impaired bone remodeling in Misty mice. J Bone Miner Res. 2013; 28. https://doi.org/10.1002/jbmr.1943 PMID: 23553822

27. Scheller EL, Doucette CR, Learman BS, Cawthorn WP, Khandaker S, Schell B, et al. Region-specific variation in the properties of skeletal adipocytes reveals regulated and constitutive marrow adipose tissues. Nat Commun. 2015; 6: 1–13. https://doi.org/10.1038/ncomms8808 PMID: 26245716

28. Takashima Y, Ma L, McKemy DD. The development of peripheral cold neural circuits based on TRPM8 expression. Neuroscience. 2010; 169: 828–842. https://doi.org/10.1016/j.neuroscience.2010.05.039 PMID: 20580783

29. Abed E, Labelle D, Martineau C, Loghin A, Moreau R. Expression of transient receptor potential (TRP) channels in human and murine osteoblast-like cells. Mol Membr Biol. 2009; 26: 146–158. https://doi.org/10.1080/09687680802612721 PMID: 19115145

30. Acharya TK, Kumar S, Tiwari N, Ghosh A, Tiwari A, Pal S, et al. TRPM8 channel inhibitor-encapsulated hydrogel as a tunable surface for bone tissue engineering. Sci Rep. 2021; 11. https://doi.org/10.1038/s41598-021-81041-w PMID: 33580126

31. Takahashi N, Matsuda Y, Sato K, De Jong PR, Bertin S, Tabeta K, et al. Neuronal TRPV1 activation regulates alveolar bone resorption by suppressing osteoclastogenesis via CGRP. Sci Rep. 2016; 6: 1–11. https://doi.org/10.1038/s41598-016-0001-8 PMID: 28442746

32. Nilius B, Voets T, Peters J. TRP channels in disease. Sci STKE. 2005; 2005: 1–10.

33. Lanske B, Rosen C. Bone Marrow Adipose Tissue: The First 40 Years. J Bone Min Res. 2017; 32: 1153–1156. https://doi.org/10.1002/jbmr.3140 PMID: 28370194

34. Wee NKY, Lorenz MR, Bekirov Y, Jacquin MF, Scheller EL. Shared autonomic pathways connect bone marrow and peripheral adipose tissues across the central neuraxis. Front Endocrinol (Lausanne). 2019; 10: 1–16. https://doi.org/10.3389/fendo.2019.00668 PMID: 31611846

35. Bautista DM, Siemens J, Glazer JM, Tsuruda PR, Basbaum AI, Stucky CL, et al. The menthol receptor TRPM8 is the principal detector of environmental cold. Nature. 2007; 448: 204–208. https://doi.org/10.1038/nature05910 PMID: 17538622

36. Shin H, Ma Y, Chanturiya T, Cao Q, Wang Y, Kadegowda AKG, et al. Lipolysis in Brown Adipocytes Is Not Essential for Cold-Induced Thermogenesis in Mice. Cell Metab. 2017; 26: 764–777.e5. https://doi.org/10.1016/j.cmet.2017.09.002 PMID: 28988822

37. Kim SN, Jung YS, Kwon HJ, Seong JK, Granneman JG, Lee YH. Sex differences in sympathetic innervation and browning of white adipose tissue of mice. Biol Sex Differ. 2016; 7: 1–13. https://doi.org/10.1186/s13293-015-0055-5 PMID: 26753091

38. Rosell M, Kaforou M, Frontini A, Okolo A, Chan YW, Nikolopoulou E, et al. Brown and white adipose tissues: Intrinsic differences in gene expression and response to cold exposure in mice. Am J Physiol—Endocrinol Metab. 2014; 306. https://doi.org/10.1152/ajpendo.00473.2013 PMID: 24549398

39. Clookey SL, Welly RJ, Shay D, Woodford ML, Fritsche KL, Rector RS, et al. Beta 3 adrenergic receptor activation rescues metabolic dysfunction in female estrogen receptor alpha-null mice. Front Physiol. 2019; 10: 1–15. https://doi.org/10.3389/fphys.2019.00001 PMID: 30723415

40. Cankar K, Music M, Finderle Z. Cutaneous microvascular response during local cold exposure—the effect of female sex hormones and cold perception. Microvasc Res. 2016; 108: 34–40. https://doi.org/10.1016/j.mvr.2016.07.006 PMID: 27430896

41. Smeester BA, O'Brien EE, Michlitsch KS, Lee JH, Beitz AJ. The relationship of bone-tumor-induced spinal cord astrocyte activation and aromatase expression to mechanical hyperalgesia and cold hypersensitivity in intact female and ovariectomized mice. Neuroscience. 2016; 324: 344–354. https://doi.org/10.1016/j.neuroscience.2016.03.030 PMID: 26995084

42. Weyer AD, Lehto SG. Development of TRPM8 antagonists to treat chronic pain and migraine. Pharmaceuticals. 2017; 10: 1–9. https://doi.org/10.3390/ph10020037 PMID: 28358322

43. Caudle RM, Caudle SL, Jenkins AC, Ahn AH, Neubert JK. Sex differences in mouse Transient Receptor Potential Cation Channel, Subfamily M, Member 8 expressing trigeminal ganglion neurons. PLoS One. 2017; 12: 1–20. https://doi.org/10.1371/journal.pone.0176753 PMID: 28472061

44. Noguchi W, Ishizuka O, Imamura T, Kurizaki Y, Yamagishi T, Yokoyama H, et al. The relationship between α1-adrenergic receptors and TRPM8 channels in detrusor overactivity induced by cold stress in ovariectomized rats. J Urol. 2013; 189: 1975–1981. https://doi.org/10.1016/j.juro.2012.10.014 PMID: 23069383

45. Kubo T, Tsuji S, Amano T, Yoshino F, Niwa Y, Kasahara K, et al. Effects of β-estradiol on cold-sensitive receptor channel TRPM8 in ovariectomized rats. Exp Anim. 2017; 66: 337–343. https://doi.org/10.1538/expanim.17-0028 PMID: 28626113

46. Winter Z, Gruschwitz P, Eger S, Touska F, Zimmermann K. Cold temperature encoding by cutaneous TRPA1 and TRPM8-carrying fibers in the mouse. Front Mol Neurosci. 2017;10. https://doi.org/10.3389/fnmol.2017.00010 PMID: 28197071

47. Feketa V V., Balasubramanian A, Flores CM, Player MR, Marrelli SP. Shivering and tachycardic responses to external cooling in mice are substantially suppressed by TRPV1 activation but not by TRPM8 inhibition. Am J Physiol—Regul Integr Comp Physiol. 2013; 305: 1040–1050. https://doi.org/10.1152/ajpregu.00296.2013 PMID: 24005250

48. Yirmiya R, Goshen I, Bajayo A, Kreisel T, Feldman S, Tam J, et al. Depression induces bone loss through stimulation of the sympathetic nervous system. Proc Natl Acad Sci U S A. 2006; 103: 16876–16881. https://doi.org/10.1073/pnas.0604234103 PMID: 17075068